Assessment of Systolic Thickening with Thallium-201 ECG-Gated Single-Photon Emission Computed Tomography: A Parameter for Local Left Ventricular Function

Teruhito Mochizuki, Kenya Murase, Yasushi Fujiwara, Shuji Tanada, Ken Hamamoto, and W. Newlon Tauxe

Department of Radiology, Second Department of Internal Medicine, Ehime University School of Medicine, Ehime, Japan; and Department of Radiology, Division of Nuclear Medicine, University of Pittsburgh School of Medicine, Pittsburgh, Pennsylvania

We measured left ventricular (LV) systolic thickening expressed as a systolic thickening ratio in 28 patients, using ^{201}Tl ECG-gated SPECT. Five normals, 15 patients with prior myocardial infarction, 5 with hypertrophic cardiomyopathy, and 3 with dilated cardiomyopathy were studied. The systolic thickening ratio was calculated as [(end-systolic—end-diastolic pixel counts) ÷ end-diastolic pixel counts], using the circumferential profile technique of both end-diastolic and end-systolic short axial images. Functional images of the systolic thickening ratio were also displayed with the "bull's-eye" method. The mean systolic thickening ratio thus calculated were as follows: normals, 0.53 ± 0.05 (mean ± 1 s.d.); non-transmural prior myocardial infarction, 0.33 ± 0.09; transmural prior myocardial infarction, 0.14 ± 0.05; hypertrophic cardiomyopathy in relatively nonhypertrophied areas, 0.56 ± 0.11; hypertrophic cardiomyopathy in hypertrophied areas, 0.23 ± 0.07; and dilated cardiomyopathy, 0.19 ± 0.02. The systolic thickening ratio analysis by gated thallium SPECT offers a unique approach for assessing LV function.

J Nucl Med 1991; 32:1496–1500

Because of its relatively long data acquisition time, ^{201}Tl ECG-gated single-photon emission computed tomography (SPECT) has not been widely used. However, this method has provided morphologic details not obtainable with non-gated SPECT and has also enabled evaluation of wall motion of the left ventricle (LV) (*1*). In addition, comparing end-systolic (ES) counts and images with end-diastolic (ED) counts and images, local systolic thickening of the LV wall could be observed as an increase in pixel counts. If one observes systolic thickening in a particular area, function and viability may be assumed even though there may be markedly decreased perfusion or absent wall motion in that area. Non-functioning but viable myocardium may be appreciated as an area of decreased perfusion with minimal systolic thickening. Analysis of systolic thickening of the LV wall offers a different approach in the evaluation of LV function than that obtained from wall motion by blood-pool study.

The goal of this study was to define a quantitative method to assess LV systolic thickening using gated thallium SPECT.

MATERIALS AND METHODS

Patients

The study group consisted of 28 subjects, including 5 normals; 15 patients with old myocardial infarction whose events occurred at least 1.5 mo before testing; 5 patients with hypertrophic cardiomyopathy having nonuniform wall thickness; and 3 patients with dilated cardiomyopathy. There were 21 males and 7 females, ages 25 to 80 yr (mean, 57).

Normal subjects were recruited from patients undergoing evaluation for other heart disease. Ages of the normal subjects ranged from 25 to 77 yr and significant coronary artery disease was ruled out by a negative clinical history and a negative exercise ECG study. Myocardial infarction was diagnosed in all patients by significantly elevated myocardial enzymes (CPK and LDH), ECG changes in the acute phase, and positive ^{99m}Tc-pyrophosphate scan (*2*) with SPECT (*3*). Diagnoses of hypertrophic cardiomyopathy and dilated cardiomyopathy were made by ECG, ultrasound, contrast left ventriculography, planar gated blood-pool study (*4–6*), and ECG-gated blood-pool SPECT (*7,8*).

Patients with prior infarction were placed into two groups based on gated thallium SPECT imaging. Eight patients whose infarcted regions had more than 50% of maximum counts in ED images (see below) were placed in the non-transmural prior myocardial infarction group and seven patients whose infarcted regions had less than 50% of maximum counts in ED images (see below) were placed in the transmural prior myocardial infarction group.

Received Jul. 31, 1990; revision accepted Mar. 6, 1991.

For reprints contact: Ken Hamamoto, MD, Department of Radiology, Ehime University School of Medicine, Shitsukawa, Shigenobu-cho, Onsen-gun, Ehime, 791-02, Japan.

Scintigraphic Technique

Patients were injected with 111–185 MBq (3–5 mCi) of ^{201}Tl-chloride at rest and imaged with a rotating gamma camera (Hitachi Gamma View-T, Tokyo, Japan) using a low-energy high-resolution collimator and interfaced to a Hitachi HARP System computer (FWHM by SPECT: 15–17 mm with ^{99m}Tc and 17–20 mm with ^{201}Tl in air, when r = 30 to 35 cm). Beginning 10 min after injection, projection data were acquired over 180° from the 45° right anterior oblique (RAO) to the 45° left posterior oblique (LPO) in 24 steps, each of which encompassed 80–100 beats with the R-R interval divided into 18–22 fractions. The mean radius of rotation was approximately 35 cm and data acquisition required 30 to 40 min. The first three fractions and the three systolic fractions were added for the reconstruction of ED and ES images, respectively. The ES fractions were defined by comparing the volume curve from the gated blood-pool study. After nine-point spatial smoothing, both ED and ES projection data were reconstructed by filtered backprojection using a Chesler filter to produce contiguous transverse slices, on a 64 × 64 matrix with a 6-mm slice thickness (1 pixel thick). Attenuation correction was not performed. Short- and long-axial images perpendicular to the cardiac axes were subsequently derived from these data.

Data Analysis

The systolic thickening ratio was calculated as [(ES—ED pixel counts) ÷ ED pixel counts] with the five-point circumferential profile summing technique in which the highest and the next four adjacent higher pixel counts on either side were added. This divides every ED and ES short-axial slice into 60 radial segments at 6° intervals from apex to base. Functional images were displayed using the "bull's-eye" method (*9,10*) (Fig. 1).

For the assessment of mean systolic thickening ratio, a 60° and three-slice region of interest (ROI) was drawn in each patient. This ROI size was chosen to limit statistical error and yet was not so large as to include normal myocardium surrounding the pathologic region. Normal and pathologic regions were defined visually using ED images of the gated thallium SPECT. In normal subjects, ROIs were drawn over the anteroseptal wall in two cases, avoiding the high anteroseptal region; over the lateral wall in one case; and over the inferior wall in two cases. In patients with prior myocardial infarction, ROIs were drawn over the area of decreased perfusion, which corresponded with the infarcted area on ^{99m}Tc-pyrophosphate SPECT, and over a normal area as a control. Since the infarcts were in various locations, pathologic and control ROIs were drawn in various regions. In patients with hypertrophic cardiomyopathy, ROIs were drawn over the areas of high and relatively normal perfusion, which corresponded grossly with hypertrophied and relatively non-hypertrophied walls respectively as shown by ultrasound. In patients with dilated cardiomyopathy, ROIs were drawn over the anterior wall.

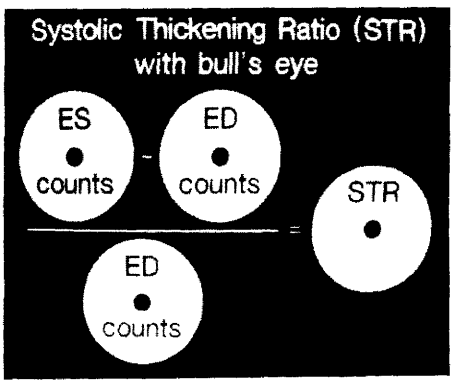

FIGURE 1. Systolic thickening ratio determination and its bull's-eye display are summarized.

Statistical Analysis

Statistical significance of differences between the mean systolic thickening ratio values of two groups was analyzed by the Student's t-test using $p < 0.05$ as a criterion for significance.

Phantom Study

For in vitro comparison, cylinders of varying heights (4, 8, 12, 16, 20, and 24 mm) with a constant diameter of 55 mm were filled with 0.37 MBq/ml (10 μCi/ml) of ^{99m}Tc. They were placed in air and upright on the imaging table so that the center of the base of the cylinder was the same as the center of rotation of the detector system used in the patients. Projection data were collected over 180° in 24 steps for 3, 6, and 9 sec each. The radius of rotation was 30 cm. After nine-point smoothing, the data were reconstructed so that the long axes of the phantoms were perpendicular to the line through the center of rotation. A 64 × 64 matrix was used and the slice thickness was 6 mm (1 pixel thick) to simulate patient data parameters. Pixel counts obtained under these conditions covered the clinical range (maximum pixel counts in ED short-axial slices ranged from 80 to 210, while in the ES slices they ranged from 80 to 280). Background setting and attenuation correction were not performed.

With profile curves at the middle of the transverse slices, the relationship between the pixel counts and the phantom thickness was investigated by the five-point summing profile method.

RESULTS

The phantom study revealed that pixel counts correlated well with the thickness at all three of the acquisition times using the five-point profile summing analysis (r = 0.995 to 0.999) (Fig. 2).

Figure 3 shows the mean systolic thickening ratio in the various ROIs for the patient studies. In normal subjects, the mean systolic thickening ratio was 0.53 ± 0.05 (mean ± 1 s.d.). In patients with non-transmural prior myocardial infarction, the mean systolic thickening ratio in the infarcted regions was 0.33 ± 0.09, while the mean systolic thickening ratio in the noninfarcted regions was 0.47 ± 0.06 ($p < 0.001$). In patients with transmural prior myocardial infarction, the mean systolic thickening ratio in the infarcted region was 0.14 ± 0.05, while the mean systolic thickening ratio in the noninfarcted regions was 0.47 ± 0.10 ($p < 0.001$). The mean systolic thickening ratio in infarcted regions of patients with non-transmural prior myocardial infarction was greater than that of patients with transmural old myocardial infarction ($p < 0.001$). In patients with hypertrophic cardiomyopathy with nonuniform wall thickness, the mean systolic thickening ratio in relatively non-hypertrophied areas was greater (0.56 ± 0.11) than that in hypertrophied areas (0.23 ± 0.07) ($p < 0.001$). In patients with dilated cardiomyopathy, the mean systolic thickening ratio was 0.19 ± 0.02.

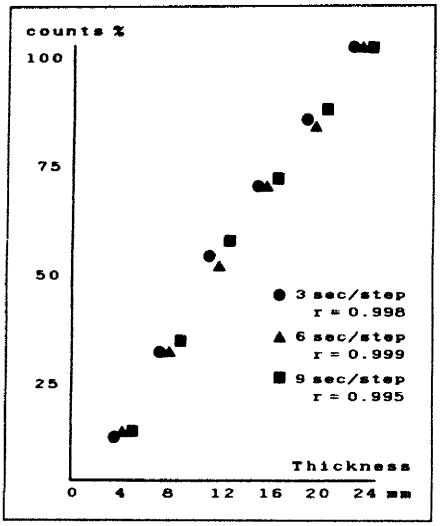

FIGURE 2. Pixel counts are plotted as a function of the thickness of phantoms at the acquisition times of 3 sec/step (○), 6 sec/step (▲), and 9 sec/step (■). There is good linear correlation at all of the three acquisition times.

Figures 4, 5, and 6 depict data from a normal subject, a patient with inferior transmural prior myocardial infarction, and a patient with hypertrophic cardiomyopathy, respectively.

DISCUSSION

Left ventricular function has been analyzed with first-pass radionuclide angiography (*11*) and with gated ^{99m}Tc-labeled blood-pool studies using both planar (*4–6*) and

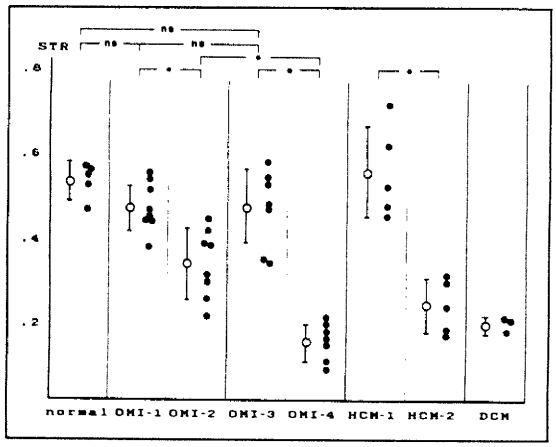

FIGURE 3. The mean systolic thickening ratio in ROIs (pathologic and control regions) are shown with a mean value and one standard deviation. OMI-1, noninfarcted area of non-transmural old myocardial infarction; OMI-2, infarcted area of non-transmural old myocardial infarction; OMI-3, noninfarcted area of transmural old myocardial infarction; OMI-4, infarcted area of transmural old myocardial infarction; HCM-1, non-hypertrophied area of hypertrophic cardiomyopathy; HCM-2, hypertrophied area of hypertrophic cardiomyopathy; DCM, dilated cardiomyopathy, anterior wall. ns: not significant. *: $p < 0.001$

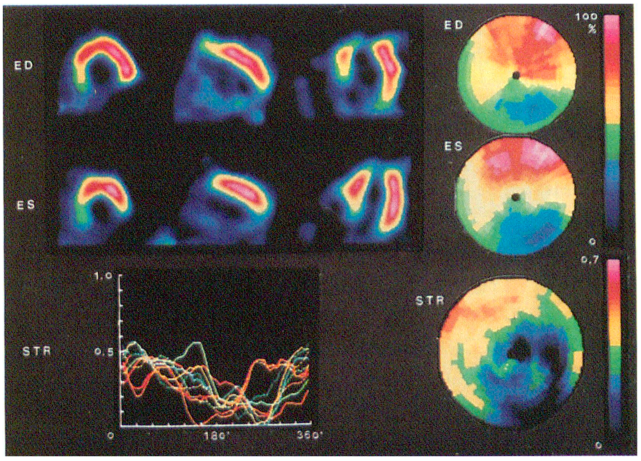

FIGURE 4. A normal subject. The ED (upper), ES (middle), and bull's-eye (upper and middle right) images show the normal perfusion and contraction. Systolic thickening ratio ranges from 0.4 to 0.7 except high antero-septal wall (see below) (lower left). Systolic thickening ratio bull's-eye display (lower right) demonstrates normal systolic thickening of the entire left ventricle. Middle to apical slices and inferior wall showed relatively high systolic thickening ratio. Low systolic thickening ratio in high anterior and high septal wall may have been affected by the potential problem discussed in the text.

SPECT (*7,8*) techniques. These methods have been widely used as routine tests to analyze the LV cavity. Thallium-201 ECG-gated myocardial SPECT has not been used for routine examination because of its long data acquisition time. However, it does offer three major inducements in analyzing the myocardium. It provides: (1) clear morphologic information (ED and ES perfusion images); (2) information about the LV wall itself including systolic thickening; and (3) information about LV wall motion (*1*).

The most important point demonstrated by our phantom study is that pixel counts relate closely to tissue

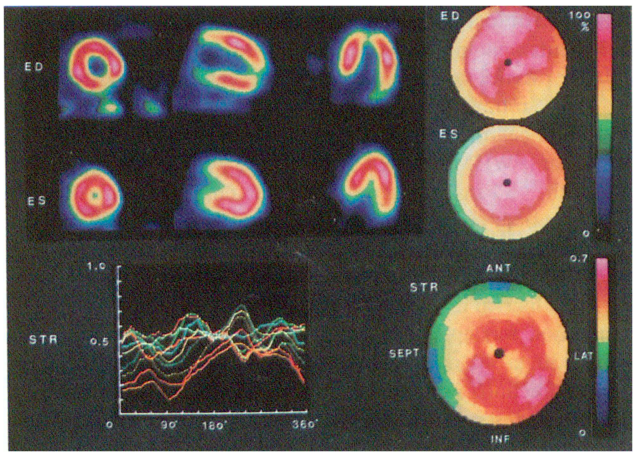

FIGURE 5. This patient had an old inferior transmural myocardial infarction. The ED, ES, and bull's-eye images show a defect in the inferior wall. Systolic thickening ratio in the infarcted area ranges from 0.0 to 0.2 suggesting no function and scar.

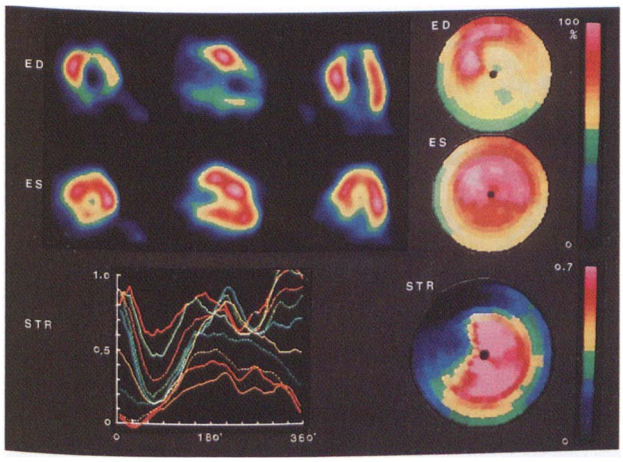

FIGURE 6. This patient had hypertrophic cardiomyopathy. The ED, ES images, and bull's-eye display show septal to high anterior hypertrophy. Systolic thickening ratio in the hypertrophied region ranges from 0.0 to 0.3. Systolic thickening ratio bull's-eye display depicts lower systolic thickening area in the nonuniform hypertrophied region, suggesting relatively poor function.

thickness. The phantom study, with object thickness of 4, 8, 12, 16, 20, and 24 mm, revealed that if radionuclide concentration and acquisition times were tested under the same conditions, the pixel counts could be substituted for the relative ED and ES wall thickness values. Therefore, when we define the systolic thickening ratio as [(ES thickness—ED thickness) ÷ ED thickness], we can estimate the systolic thickening ratio as [(ES pixel counts—ED pixel counts) ÷ ED pixel counts].

Inaccuracy of the systolic thickening ratio measurement may have been caused by the following potential problems. The slope between 4 and 12 mm was a little greater than that between 12 and 24 mm. This may explain why the systolic thickening ratio in the thinner wall (lower perfusion area) seemed to be slightly higher than that in the thicker wall (higher or normal perfusion area). Very low pixel counts, especially in the area of transmural prior myocardial infarction, may have caused the relatively large error in calculating the systolic thickening ratio. In the inferior wall, the ES counts might be measured slightly higher than the ED counts, perhaps because of the lower attenuation of the contracted LV volume. However, there was also attenuation of the thickened anterior wall, which would reduce this problem. A point defined in the ED image may differ from that defined in the ES image, i.e., it may go to the next slice during contraction. In the middle of the left ventricle, the mismatch seemed minimum. However, in the apex and base, it may be significant.

In this study, we could not compare the systolic thickening ratio by gated thallium SPECT with other modalities, i.e., ultrasound, left ventriculography, gated blood-pool SPECT, PET, or MRI. Of these, left ventriculography and gated blood-pool SPECT are not suitable for comparison, since there may be a discordance between wall motion and systolic thickening. Ultrasound also does not seem suitable for comparison, since it is difficult to define the whole LV short-axial images accurately and objectively. ECG-gated MRI may be a better modality for comparison if image quality is high enough. Yamashita et al. (*12*) have analyzed systolic thickening using ECG-gated PET in 9 normal subjects and 16 patients with coronary artery disease. In their study, systolic thickening was measured in three transverse slices of the left ventricle. They reported that mean values of normal subjects in eight regions of the middle slice ranged from 39.8% to 66.1% (mean, 53.2%), which was very close to our results (0.53%). ECG-gated PET may quantify systolic thickening ratio more accurately than ECG-gated SPECT, however, SPECT can examine the entire LV wall easily, utilizing short-axial images, which provided us with bull's-eye functional images of the systolic thickening ratio. A drawback of the bull's-eye method is in the evaluation of the apex. Visual and systolic thickening ratio analyses using the long-axial images are recommended in this instance.

With our method, we could confirm various degrees of systolic thickening in infarcted areas. Evaluation of residual LV function and viability in the infarcted area is important when making a decision as to whether percutaneous transluminal coronary angioplasty (*13,14*) or coronary artery bypass grafting (*15–17*). For the evaluation of ischemia, stress-redistribution ^{201}Tl myocardial scintigraphy (*18–22*) has been recommended; however, it is not sufficient for the evaluation of tissue viability. Several authors have reported that some persistent defects on 2–5-hr delayed scans are viable and reversible (*23–28*). Therefore, the "rest" ^{201}Tl study seems to be better for the evaluation of viability. In our study, the rest gated thallium SPECT was of greater value than the non-gated since it provided both clearer perfusion and LV function images.

In patients with hypertrophic cardiomyopathy and dilated cardiomyopathy, the evaluation of morphologic details, local LV wall motion, and systolic thickening ratio with gated thallium SPECT, may be useful both for patient management and for research purposes.

Although gated thallium SPECT has not been widely used for routine examination because of its relatively long data acquisition time (30–40 min), it should be considered in light of the many advantages discussed above. To assess the predictive power of systolic thickening ratio analysis for evaluating viability (potential to recover function), further study including comparison with other modalities (MRI or PET) and follow up after intervention is required. Although this study was performed with ^{201}Tl, the method will be applicable with the newer ^{99m}Tc agents (*29–32*), which will significantly shorten data acquisition time and make the systolic thickening ratio analysis more practical.

ACKNOWLEDGMENTS

The authors gratefully acknowledge the assistance of Jeffrey Dobkin, MD, Ms. Meg Sachse, and Ms. Judith K. Holden for preparation of the manuscript.

REFERENCES

1. Mochizuki T, Murase K, Tanada S, et al. Clinical evaluation of the thallium-201 ECG-gated myocardial SPECT [Abstract]. *J Nucl Med* 1989;30:864.
2. Parkey RW, Bonte FJ, Meyer SL, et al. A new method for radionuclide imaging of acute myocardial infarction in humans. *Circulation* 1974;50:540–546.
3. Fujiwara Y, Mochizuki T, Itoh T, et al. Quantitative analysis of acute myocardial infarction using single photon emission computed tomography using technetium-99m-pyrophosphate. *J Cardiogr* 1986;16:555–562.
4. Strauss HW, Zaret BL, Hurley PJ, Natarajan TK, Pitt B. A scintigraphic method for measuring left ventricular ejection in man without cardiac catheterization. *Am J Cardiol* 1971;28:575–580.
5. Burow RD, Strauss HW, Singleton R, et al. Analysis of left ventricular function with multiple gated acquisition cardiac blood-pool imaging. Comparison to contrast angiography. *Circulation* 1977;56:1024–1028.
6. Qureshi S, Wagner HN, Alderson PO, et al. Evaluation of left ventricular function in normal persons and patients with heart disease. *J Nucl Med* 1978;19:135–141.
7. Moore ML, Murphy PH, Burdine JA. ECG-gated emission computed tomography of the cardiac blood pool. *Radiology* 1980;134:223–235.
8. Tamaki N, Mukai T, Ishii Y, et al. Multiaxial tomography of heart chambers by gated blood-pool emission computed tomography using a rotating gamma camera. *Radiology* 1983;147:547–554.
9. Garcia EV, Train KV, Maddahi J, et al. Quantification of rotational thallium-201 myocardial tomography. *J Nucl Med* 1985;26:17–26.
10. DePasquale EE, Nody AC, DePuey EG, et al. Quantitative rotational thallium-201 tomography for identifying and localizing coronary artery disease. *Circulation* 1988;77:316–327.
11. Hecht HS, Mirell SG, Rollet EL, Blahd WH. Left ventricular ejection fraction and segmental wall motion by peripheral first-pass radionuclide angiography. *J Nucl Med* 1978;19:17–23.
12. Yamashita K, Tamaki N, Yonekura Y, et al. Quantitative analysis of regional wall motion by gated myocardial positron tomography: validation and comparison with left ventriculography. *J Nucl Med* 1989;30:1775–1786.
13. Gruntzig AR, Senning A, Siegenthalter WE. Nonoperative dilatation of coronary artery stenosis. Percutaneous transluminal coronary angioplasty. *N Eng J Med* 1979;301:61–68.
14. Gruentzig AR, King III SB, Schlumpf M, Siegenthaler W. Long-term follow-up after percutaneous transluminal coronary angioplasty: the early Zurich experience. *N Engl J Med* 1987;316:1127–1132.
15. Green GE, Spencer FC, Tice DA, Stertzer SH. Arterial and venous microsurgical bypass grafts for coronary artery disease. *J Thorac Cardiovasc Surg* 1970;60:491–503.
16. Tyras DH, Barner HB, Kaiser GC, Codd JE, Pennington DG, Willman VL. Bypass grafts to the left anterior descending coronary artery. *J Thorac Cardiovasc Surg* 1980;80:327–333.
17. Jones JW, Ochsner JL, Mills NL, Hughes L. Clinical comparison between patients with saphenous vein and internal mammary artery as a coronary graft. *J Thorac Cardiovasc Surg* 1980;80:334–341.
18. Pohost GM, Alpert NM, Ingwall JS, Strauss HW. Thallium redistribution: mechanisms and clinical utility. *Semin Nucl Med* 1980;10:70–93.
19. Maddahi J, Garcia EV, Berman DS, Waxman A, Swan HJC, Forrester J. Improved noninvasive assessment of coronary artery disease by quantitative analysis of regional stress myocardial distribution and washout of thallium-201. *Circulation* 1981;64:924–935.
20. Rozanski A, Berman DS, Gray R, et al. Use of thallium-201 redistribution scintigraphy in the preoperative differentiation of reversible and nonreversible myocardial asynergy. *Circulation* 1982;64:936–944.
21. Staring MR, Walsh RA, Dehmer GJ, Lasher JC, Blumhardt R. Value of tomographic thallium-201 imaging in patients with chest pain following coronary artery bypass grafting. *Clin Nucl Med* 1987;12:134–139.
22. Valette H, Bourguignon MH, Guludec DL, et al. ECG-gated thallium-201 myocardial images: value in detecting multivessel disease in patients on anti-anginal therapy 1–3 months after myocardial infarction. *Eur J Nucl Med* 1987;13:551–556.
23. Gutman J, Berman DS, Freeman M, et al. Time to completed redistribution of thallium-201 in exercise myocardial scintigraphy. *Am Heart J* 1983;106:989–995.
24. Ziessman HA, Sigler CJ, Wells TM, et al. Utility of delayed 24-hour redistribution on SPECT thallium-201 myocardial perfusion studies [Abstract]. *J Nucl Med* 1988;29:769.
25. Hecht HS, Andreae G, Myler RK, Chin H. The role of 24 hour tomographic thallium-201 myocardial imaging in revascularization [Abstract]. *J Nucl Med* 1988;29:769.
26. Rocco T, Dilsizian V, Maltais F, Strauss HW, Boucher CA, McKusick KA. Thallium reinjection after delayed imaging demonstrates fill-in to regions with "fixed" defects [Abstract]. *J Nucl Med* 1988;29:769.
27. Tamaki N, Yonekura Y, Yamashita K, et al. Value of rest-stress myocardial positron tomography using nitrogen-13-ammonia for the preoperative prediction of reversible asynergy. *J Nucl Med* 1989;30:1302–1310.
28. Brunken RC, Kottou S, Nienaber CA, et al. PET detection of viable tissue in myocardial segments with persistent defects at T1-201 SPECT. *Radiology* 1989;172:65–73.
29. Sia STB, Holman BL. Dynamic myocardial imaging in ischemic heart disease. Use of technetium-99m isonitriles. *Am J Cardiol Imaging* 1987;1:125–131.
30. Okada RD, Glover D, Gaffney T, Williams S. Myocardial kinetics of technetium-99m-hexakis-2-methoxy-2-mythylpropyl-isonitrile. *Circulation* 1988;77:491–498.
31. McGhie I, Faber TL, Akers MS, Kahn JK, Corbett JR. Assessment of the relationship between ventricular function and perfusion in patients with myocardial infarction using gated tomographic imaging with Tc-99m-MIBI and radionuclide ventriculography [Abstract]. *J Nucl Med* 1989;30:801.
32. Gerundini P, Maffioli L. Cationic complexes of technetium for myocardial imaging. *J Nucl Med* 1989;30:1415–1419.